DOI: 10.1002/ejoc.200500708

Effect of the Leaving Group on the Rate and Mechanism of the Palladium-Catalyzed Isomerization of Cyclic Allylic Benzoates in Allylic Substitutions

Christian Amatore,*[a] Anny Jutand,*[a] Laure Mensah,[a] Gilbert Meyer,[a] Jean-Claude Fiaud,*,[b] and Jean-Yves Legros[b]

Keywords: Palladium / Allylic benzoates / Allylic complexes / Mechanism / Kinetics / Isomerization

In chloroform, the reaction of *cis*-5-phenylcyclohex-2-enyl 4-Z-benzoate (*cis*-**1**$_Z$, Z = NO_2, Cl, H, Me, MeO) with Pd^0 complexes ligated to PPh_3 is reversible and proceeds with isomerization at the allylic position. The rate of isomerization of *cis*-**1**$_Z$ to *trans*-**1**$_Z$ depends on the catalytic precursor: $Pd^0(PPh_3)_4 > \{Pd^0(dba)_2 + 2PPh_3\}$ in agreement with an S_N2 mechanism in the rate-determining isomerization of the cationic (η^3-allyl)palladium complexes formed in the oxidative addition. For a given precursor, the rate of isomerization of *cis*-**1**$_Z$ to *trans*-**1**$_Z$ also depends on the substituent Z, i.e., on the leaving group. The isomerization rate follows the same order as the leaving group properties: 4-NO_2–C_6H_4-CO_2^- > 4-Cl–C_6H_4-CO_2^- > C_6H_5-CO_2^- > 4-Me–C_6H_4-CO_2^- > 4-MeO–C_6H_4-CO_2^-. The same tendency is found for the equilibrium constant between the neutral *cis*-**1**$_Z$ and the cationic (η^3-allyl)palladium complex in DMF. The higher the concentration of the cationic (η^3-allyl)palladium complex, the faster the isomerization of *cis*-**1**$_Z$ to *trans*-**1**$_Z$ is. The isomerization of *cis*-**1**$_Z$ to *trans*-**1**$_Z$ and that of the cationic (η^3-allyl)palladium complexes are at the origin of the lack of stereospecificity observed in catalytic nucleophilic allylic substitutions. These isomerizations are affected by both the leaving groups and the Pd^0 precursors, which therefore are not "innocent" but may play an important role in palladium-catalyzed nucleophilic substitutions.

Introduction

The palladium-catalyzed nucleophilic substitution on allylic carboxylates is a well-documented synthetic reaction.[1] Investigations of allylic substitutions on substituted cyclic allylic carboxylates have brought interesting insights into the mechanism of the successive steps of these catalytic reactions (Scheme 1).[2,3]

The oxidative addition of a substituted cyclic allylic carboxylate to a palladium(0) complex, which generates a cationic (η^3-allyl)palladium complex, was established to proceed by an inversion of configuration,[3] whereas the nucleophilic attack proceeds: i) by inversion of configuration in the case of soft or stabilized nucleophiles, Nu_S, which attack the allylic ligand with an overall retention of configuration or ii) by retention of configuration in the case of hard or nonstabilized nucleophiles, Nu_H, which attack the palladium center, resulting in an overall inversion of configuration (Scheme 1).[2,3]

According to these mechanisms, catalytic substitutions on one isomer should proceed either by retention or by inversion of configuration according to the nature of the nucleophile, and the reactions should be stereospecific. However, a loss of stereospecificity is often observed. This was first accounted for by isomerization of the starting cyclic allylic carboxylates,[4] and then by an isomerization of the cationic (η^3-allyl)palladium by an S_N2 mechanism induced by the palladium(0) catalyst, as already proposed in the acyclic series.[5] In this context, we have also established that the oxidative addition of cyclic allylic carbonates is reversible and proceeds by an isomerization at the allylic carbon, via the isomerization of the cationic (η^3-allyl)palladium by an S_N2 mechanism (Scheme 2, Scheme 3).[5f]

Palladium-catalyzed asymmetric allylic substitution may also depend on the leaving group attached to the allylic moieties.[1d,5d,6]

We wish to report here a mechanistic study of the oxidative addition of cyclic allylic *para*-Z-substituted benzoates (*cis*-**1**$_Z$) with Pd^0 complexes, with a focus on the effect of the leaving group on the kinetics, thermodynamics and stereochemistry of the oxidative addition. To the best of our knowledge, no kinetic or thermodynamic data on the oxidative addition dealing with the effect of the leaving group on the palladium-catalyzed isomerization of allylic carboxylates are available in the literature.

[a] Ecole Normale Supérieure, Département de Chimie, UMR CNRS-ENS-UPMC 8640,
24, Rue Lhomond, 75231 Paris Cedex 5, France
Fax: +33-1-44323325
E-mail: Anny.Jutand@ens.fr
[b] ICMO, Bat. 420, Université Paris XI,
91405 Orsay, France

Supporting information for this article is available on the WWW under http://www.eurjoc.org or from the author.

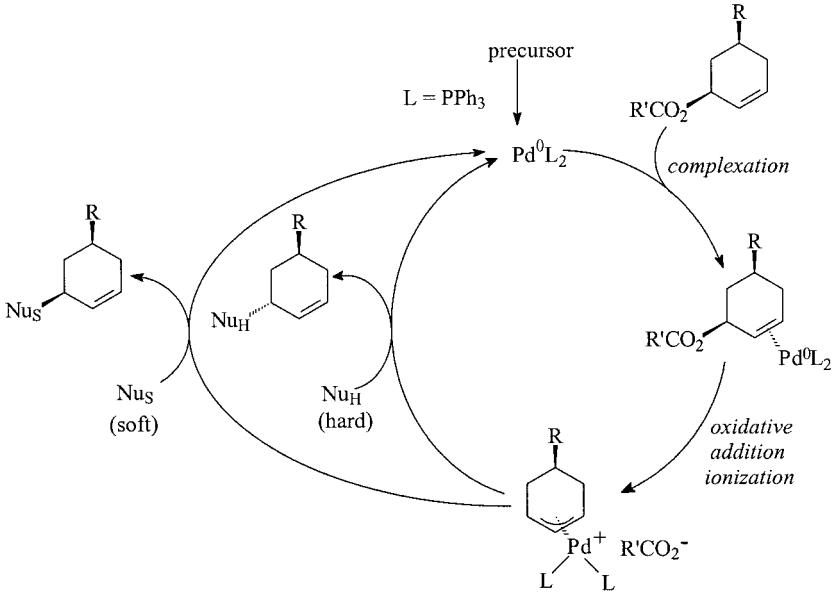

Scheme 1.

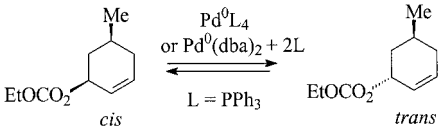

Scheme 2.

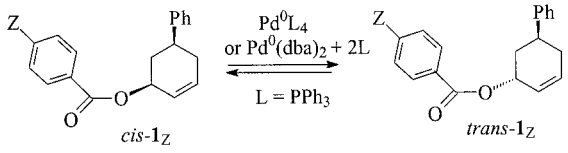

Scheme 4.

Results and Discussion

Mechanism of the Reaction of *cis*-5-Phenylcyclohex-2-enyl Benzoate (*cis*-$\mathbf{1}_H$) with Pd^0 Complexes: Influence of the Catalytic Precursor

Reversibility of the Oxidative Addition and Isomerization

The reaction of *cis*-$\mathbf{1}_H$ (40 mM) with two precursors of palladium(0) [$Pd^0(PPh_3)_4$ (20 mM) or $Pd^0(dba)_2$ (20 mM)] associated with two equiv. of PPh_3 (40 mM), was monitored by ^1H NMR spectroscopy in $CDCl_3$. The ^1H NMR signals of *trans*-$\mathbf{1}_H$ were soon detected, and were found to increase with time at the expense of those of *cis*-$\mathbf{1}_H$, until the thermodynamic equilibrium was reached: [*trans*-$\mathbf{1}_H$]/[*cis*-$\mathbf{1}_H$] = 54:46 (Scheme 4).

It is worthwhile to note that the ^1H NMR spectrum exhibited only the signals of *cis*-$\mathbf{1}_H$ and *trans*-$\mathbf{1}_H$. No other signals could be detected, in particular those which would have characterized the cationic complexes, *trans*-$\mathbf{2}^+$ or *cis*-$\mathbf{2}^+$, generated in the reaction of *cis*-$\mathbf{1}_H$ with the Pd^0 complexes. This suggests that for the experimental conditions indicated above, the relative abundance of the *cis*-**1**/*trans*-**1** pair vs. the cationic *trans*-$\mathbf{2}^+$/*cis*-$\mathbf{2}^+$ pair lies in favor of the starting compounds. The equilibrium constant between *trans*-$\mathbf{1}_H$ and *cis*-$\mathbf{1}_H$ has been determined: K = [*trans*-$\mathbf{1}_H$]/[*cis*-$\mathbf{1}_H$] = 1.17 ($CDCl_3$, 25 °C).

The percentage of *trans*-$\mathbf{1}_H$ in the mixture *trans*-$\mathbf{1}_H$ + *cis*-$\mathbf{1}_H$ was plotted against time for the two catalytic precursors (Figure 1).

According to Figure 1, the isomerization *cis*-$\mathbf{1}_H$/*trans*-$\mathbf{1}_H$ was faster when $Pd^0(PPh_3)_4$ was used as the precursor than

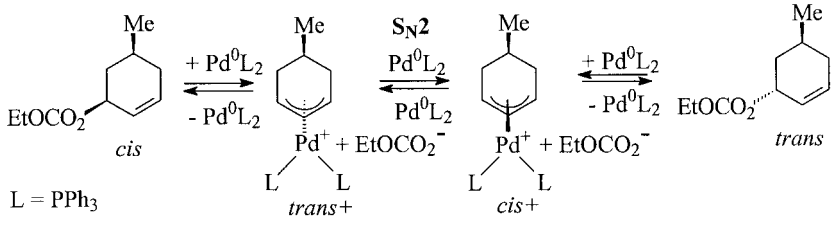

Scheme 3.

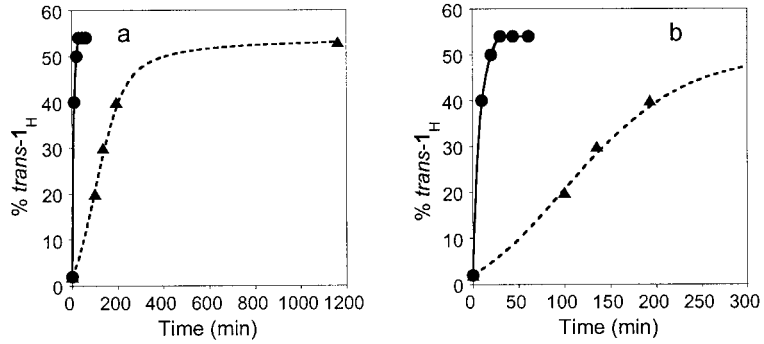

Figure 1. a) (— and solid circles): percentage of *trans*-$\mathbf{1}_H$ formed in the reaction of *cis*-$\mathbf{1}_H$ (40 mM) with the Pd^0 complex generated from $Pd^0(PPh_3)_4$ (20 mM) in $CDCl_3$ at 25 °C, as determined by ^1H NMR spectroscopy. (– – – and solid triangles): percentage of *trans*-$\mathbf{1}_H$ formed in the reaction of *cis*-$\mathbf{1}_H$ (40 mM) with the Pd^0 complex generated from $Pd^0(dba)_2$ (20 mM) and PPh_3 (40 mM) in $CDCl_3$ at 25 °C. b) Same data as in Figure 1 (a) from 0 to 300 min.

with $Pd^0(dba)_2 + 2PPh_3$. This situation was already encountered with a cyclic allylic carbonate (Scheme 2), and was rationalized by invoking a mechanism involving the isomerization of the cationic complexes by an S_N2 mechanism (Scheme 3).[5f] The rate of isomerization must increase when the $Pd^0(PPh_3)_2$ concentration is made higher, since this low-ligated intermediate is directly involved in the bimolecular rate-determining step. We know from our previous work that for identical concentrations of $Pd^0(PPh_3)_3$ [the major complex generated from $Pd^0(PPh_3)_4$] and $Pd^0(dba)(PPh_3)_2$ [the major complex generated from $Pd^0(dba)_2 + 2PPh_3$], the $Pd^0(PPh_3)_2$ concentration in the equilibrium of Scheme 5 is lower than in the equilibrium of Scheme 6 ($K'_0 > K_0$).[7]

$$Pd^0(dba)L_2 \underset{}{\overset{K_0}{\rightleftharpoons}} Pd^0L_2 + dba$$

Scheme 5.

$$Pd^0L_3 \overset{K'_0}{\rightleftharpoons} Pd^0L_2 + L$$

Scheme 6.

The kinetics of the isomerization *cis*-$\mathbf{1}_H$/*trans*-$\mathbf{1}_H$ were thus thoroughly investigated to confirm the S_N2 mechanism proposed in Scheme 7.

Kinetics of the Isomerization cis-1$_H$/trans-1$_H$

Since the cationic species are not observable, they are under steady state conditions. The overall isomerization may be represented by the formal equation in Scheme 8 as the results of three successive equilibria (Scheme 7), where k_+ and k_- are apparent rate constants.

$$cis\text{-}\mathbf{1}_Z + Pd^0L_2 \underset{k_-}{\overset{k_+}{\rightleftharpoons}} trans\text{-}\mathbf{1}_Z + Pd^0L_2 \qquad K = k_+/k_-$$
$$L = PPh_3$$

Scheme 8.

The kinetic law for the overall isomerization process (Scheme 8) is given in Scheme 9 (x= [*cis*-$\mathbf{1}_Z$]/C_0 at t; C_0 = initial concentration of *cis*-$\mathbf{1}_Z$).

$$d[cis\text{-}\mathbf{1}_Z]/dt = -k_+[cis\text{-}\mathbf{1}_Z][Pd^0L_2] + k_-[trans\text{-}\mathbf{1}_Z][Pd^0L_2]$$

$$\text{with } [cis\text{-}\mathbf{1}_Z] + [trans\text{-}\mathbf{1}_Z] = C_0 \text{ and } [trans\text{-}\mathbf{1}_Z]/[cis\text{-}\mathbf{1}_Z] = K$$

After integration, one gets the following kinetic law :

$$\ln [x(K+1) - 1] - \ln K = -(k_+ + k_-)[Pd^0L_2]\, t = -k_{obs}\, t$$

Scheme 9.

The plot of $\{\ln[x(K + 1) - 1] - \ln K\}$ against time was linear for the catalytic precursors, $Pd^0(PPh_3)_4$ (Figure 2, a) and $Pd^0(dba)_2 + 2PPh_3$ (Figure 2, b), as predicted by the kinetic law reported in Scheme 9. This validates the kinetic framework shown in Scheme 8.

The value of $k'_{obs} = 2.2 \times 10^{-3}\ s^{-1}$ for $Pd^0(PPh_3)_4$ was determined from the slope of the straight line (Figure 2, a). The rate constant $k_{obs} = 1.5 \times 10^{-4}\ s^{-1}$ for $Pd^0(dba)(PPh_3)_2$ (Figure 2, b).[8a] Two different values for the observed rate constants were obtained, depending on the catalytic precursor. This indicates that the rate of isomerization depends on the concentration of the active $Pd^0(PPh_3)_2$, which in turn depends on the precursor for identical Pd^0 overall concentrations.[7] This is again in full agreement with the rate law

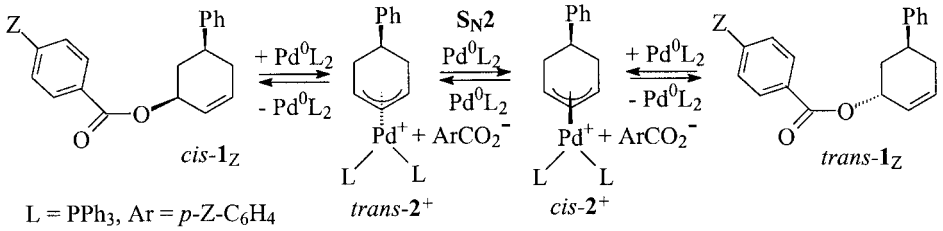

Scheme 7.

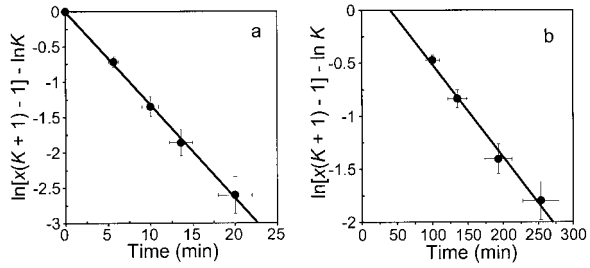

Figure 2. a) Kinetics of the isomerization of *cis*-$\mathbf{1}_H$ to *trans*-$\mathbf{1}_H$ catalyzed by the Pd^0 complex generated from $Pd^0(PPh_3)_4$ (20 mM) in $CDCl_3$ at 25 °C. Plot of $\ln[x(K + 1) - 1] - \ln K$ against time; $x = [cis\text{-}\mathbf{1}_Z]/C_0$ at t, C_0 = initial concentration of *cis*-$\mathbf{1}_H$ = 40 mM, K = equilibrium constant between *cis*-$\mathbf{1}_H$ and *trans*-$\mathbf{1}_H$ determined from the data in part a of of Figure 1. b) Same as inpart a of Figure 2 for the kinetics of isomerization *cis*-$\mathbf{1}_H$ (C_0 = 40 mM) to *trans*-$\mathbf{1}_H$ catalyzed by the Pd^0 complex generated from $Pd^0(dba)_2$ (20 mM) and PPh_3 (40 mM) in $CDCl_3$ at 25 °C.

given in Scheme 9 and the S_N2 mechanism proposed in Scheme 7.

From the experimental values of k'_{obs} and k_{obs}, one deduces that $k'_{obs}/k_{obs} = [Pd^0(PPh_3)_2]_{equil6}/[Pd^0(PPh_3)_2]_{equil5} = 14$, which gives the ratio of the concentration of $[Pd^0(PPh_3)_2]_{equil6}$ and $[Pd^0(PPh_3)_2]_{equil5}$ in their equilibria with their respective precursors in $CDCl_3$ (Scheme 5 and Scheme 6). The value of the equilibrium constant K_0 (Scheme 5) is not known in $CDCl_3$, but has been determined independently in DMF at 25 °C ($K_0 = 1.5\times10^{-5}$ M) with $[Pd^0(PPh_3)_2]_{equil5} = 1.5\times10^{-5}$ M.[8b] As far as $Pd^0(PPh_4)_4$ is concerned, the equilibrium constant K'_0 (Scheme 6) could not be determined independently. However, in a previous work, we established that, for identical concentrations of PhI and the Pd^0 precursor, the oxidative addition was 8.6 times faster with $Pd^0(PPh_4)_4$ than with $Pd^0(dba)(PPh_3)_2$ in DMF at 20 °C,[7] thus $K'_0/K_0 = 8.6$ (DMF, 20 °C). This gives a ratio of $[Pd^0(PPh_3)_2]_{equil6}/[Pd^0(PPh_3)_2]_{equil5} = 8.6$ (DMF, 20 °C) which is not far from the value of 13, obtained above in this work in $CDCl_3$ at 25 °C. The values of k_+ and k_- have been estimated from the estimated value of $k_+ + k_-$ associated with the value of $K = k_+/k_- = 1.17$ determined in this work.[8c]

This kinetic study establishes that the oxidative addition of the cyclic allylic benzoate (*cis*-$\mathbf{1}_H$) with Pd^0 complexes ligated by PPh_3 is reversible and proceeds with isomerization at the allylic position via isomerization of the cationic complexes $\mathbf{2}^+$ by an S_N2 mechanism (Scheme 7).

Thermodynamics of the Oxidative Addition

The thermodynamics of the overall equilibrium (Scheme 10) in which the cationic complex *trans*-$\mathbf{2}^+$ was formed by reaction of *cis*-$\mathbf{1}_H$ with $Pd^0(dba)(PPh_3)_2$ generated from $Pd^0(dba)_2$ (1 mM) and 2 equiv. of PPh_3 (2 mM) was investigated by UV spectroscopy in DMF at 25 °C. DMF was used as solvent instead of $CHCl_3$ because it allowed the observation of cationic complexes $\mathbf{2}^+$ by conductivity measurements (free ions in DMF,[10] vide infra in Figure S6 in the Supporting Information), whereas ion pairs are produced in THF[11] or $CHCl_3$, and no conductivity could be measured in $CDCl_3$. The absorbance of $Pd^0(dba)(PPh_3)_2$ at λ_{max}= 400 nm[9] decreased and stabilized at different values upon successive additions of *cis*-$\mathbf{1}_H$ (n equiv.) (Figure 3), as in an equilibrium (Scheme 10). The equilibrium constant $K_0K_1 = C_0x^2(1+x)/[(n - x)(1 - x)]$ was determined by plotting $x^2(1 + x)/(n - x)$ vs. $(1 - x)$ (see Figure S1, Supporting Information) [$(1 - x)$ = molar fraction of $Pd^0(dba)(PPh_3)_2$ in the equilibrium, $(1 - x) = (D_{equil} - D_{lim})/(D_0 - D_{lim})$ with D_{equil} = absorbance of $Pd^0(dba)(PPh_3)_2$ at the equilibrium in the presence of n equiv. of *cis*-$\mathbf{1}_H$, D_{lim} = residual absorbance, D_0 = initial absorbance]. K_0K_1 was determined to be 7.2×10^{-6} M (DMF, 25 °C).

$$Pd^0(dba)L_2 \overset{K_0}{\rightleftharpoons} Pd^0L_2 + dba \qquad L = PPh_3$$

$$cis\text{-}\mathbf{1}_Z/trans\text{-}\mathbf{1}_Z + Pd^0L_2 \overset{K_1}{\rightleftharpoons} trans\text{-}\mathbf{2}^+/cis\text{-}\mathbf{2}^+ + ArCO_2^-$$

Overall equilibrium

$$cis\text{-}\mathbf{1}_Z/trans\text{-}\mathbf{1}_Z + Pd^0(dba)L_2 \overset{K_0K_1}{\rightleftharpoons} trans\text{-}\mathbf{2}^+/cis\text{-}\mathbf{2}^+ + ArCO_2^- + dba$$

Scheme 10.

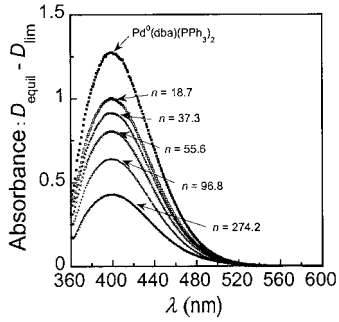

Figure 3. UV spectrum of a solution of $Pd(dba)_2$ (1 mM) and PPh_3 (2 mM) in the presence of n equiv. of *cis*-$\mathbf{1}_H$ at 25 °C. D_{equil} = absorbance of $Pd(dba)(PPh_3)_2$ at equilibrium in the presence of n equiv. of *cis*-$\mathbf{1}_H$; D_{lim} = residual absorbance observed after addition of PhI (5 mM)].

The same procedure was used to determine the overall equilibrium constant K'_0K_1 for the formation of the cationic complex *trans*-$\mathbf{2}^+$ by reaction of *cis*-$\mathbf{1}_H$ with $Pd^0(PPh_3)_3$ generated from $Pd^0(PPh_3)_4$ (1 mM) in DMF (Scheme 11 and Figures S2a and S2b).

$$K'_0K_1 = 2.4\times10^{-5}\ M\ (DMF, 25\ °C)$$

$$Pd^0L_3 \overset{K'_0}{\rightleftharpoons} Pd^0L_2 + L \qquad L = PPh_3$$

$$cis\text{-}\mathbf{1}_Z/trans\text{-}\mathbf{1}_Z + Pd^0L_2 \overset{K_1}{\rightleftharpoons} trans\text{-}\mathbf{2}^+/cis\text{-}\mathbf{2}^+ + ArCO_2^-$$

Overall equilibrium

$$cis\text{-}\mathbf{1}_Z/trans\text{-}\mathbf{1}_Z + Pd^0L_3 \overset{K'_0K_1}{\rightleftharpoons} trans\text{-}\mathbf{2}^+/cis\text{-}\mathbf{2}^+ + ArCO_2^- + L$$

Scheme 11.

Mechanism of the Reaction of *cis*-5-Phenylcyclohex-2-enyl 4-Z-Substituted Benzoate (*cis*-$\mathbf{1}_Z$) with Pd^0 Complexes: Influence of the Leaving Group

The effect of the leaving group on the kinetics of the palladium-catalyzed isomerization of *cis* cyclic allylic *para*-

Z-substituted benzoates (*cis*-$\mathbf{1}_Z$) has been investigated for Z = NO_2, Cl, Me and OMe, with the two precursors $Pd^0(dba)_2$ + $2PPh_3$ and $Pd^0(PPh_3)_4$ in $CDCl_3$, under the same experimental conditions as for Z = H (Scheme 4). *para*-Z-Substituted benzoates are good leaving groups and consequently poor nucleophiles when Z is a good electron-withdrawing group. The kinetics of the isomerization of *cis*-$\mathbf{1}_Z$ to *trans*-$\mathbf{1}_Z$ was followed by ^1H NMR, as above for *cis*-$\mathbf{1}_H$ [Figure 4 for $Pd^0(dba)_2$ + $2PPh_3$ and Figure 5 for $Pd^0(PPh_3)_4$].

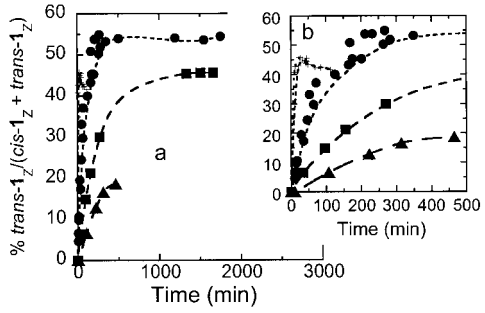

Figure 4. Percentage of *trans*-$\mathbf{1}_Z$ formed in the reaction of *cis*-$\mathbf{1}_Z$ (40 mM) with the Pd^0 complex generated from $Pd^0(dba)_2$ (20 mM) and PPh_3 (40 mM) in $CDCl_3$ at 25 °C, as determined by ^1H NMR spectroscopy. (+) Z = NO_2; (●) Z = Cl; (■) Z = Me; (▲) Z = OMe.

The observed rate constants k_{obs} (Scheme 9) have been determined as for *cis*-$\mathbf{1}_H$. For example, the determination of k_{obs} for the isomerization of *cis*-$\mathbf{1}_{OMe}$ (40 mM) to *trans*-$\mathbf{1}_{OMe}$ catalyzed by $Pd^0(PPh_3)_4$ (20 mM) is shown in Figure 6. The other kinetic curves are shown in the Supporting Information (Figures S3 and S4). The values of the rate constants k_{obs} and equilibrium constants K are collected in Table 1. The values of k_+ and k_- have been estimated.[8d]

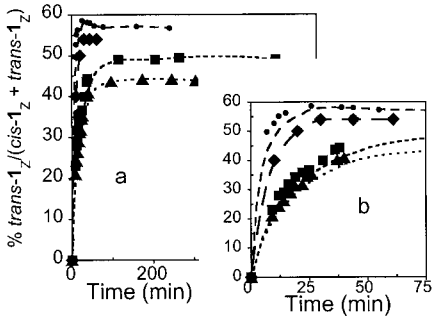

Figure 5. Percentage of *trans*-$\mathbf{1}_Z$ formed in the reaction of *cis*-$\mathbf{1}_Z$ (40 mM) with the Pd^0 complex generated from $Pd^0(PPh_3)_4$ (20 mM) in $CDCl_3$ at 25 °C, as determined by ^1H NMR spectroscopy. (●) Z = Cl; (♦) Z = H; (■) Z = Me; (▲) Z = OMe.

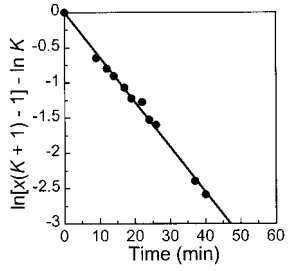

Figure 6. a) Kinetics of the isomerization *cis*-$\mathbf{1}_{OMe}$ to *trans*-$\mathbf{1}_{OMe}$ catalyzed by the Pd^0 complex generated from $Pd^0(PPh_3)_4$ (20 mM) in $CDCl_3$ at 25 °C. Plot of $\ln[x(K + 1) - 1] - \ln K$ against time (x = [*cis*-$\mathbf{1}_{OMe}$]/C_0 at t, C_0 = initial concentration of *cis*-$\mathbf{1}_{OMe}$ = 40 mM, K = equilibrium constant between *cis*-$\mathbf{1}_{OMe}$ and *trans*-$\mathbf{1}_{OMe}$).

The values of the equilibrium constants K_0K_1 and K'_0K_1 (Scheme 10, Scheme 11) have also been determined by UV spectroscopy in DMF as above for *cis*-$\mathbf{1}_H$.[12] When trying to determine the equilibrium constant K_0K_1 for *cis*-$\mathbf{1}_{OMe}$

Table 1. Kinetic and thermodynamic data for the isomerization of *cis*-$\mathbf{1}_Z$ to *trans*-$\mathbf{1}_Z$ catalyzed by Pd^0 complexes in $CDCl_3$ at 25 °C (for the definition of K and k_{obs}, see Scheme 8 and Scheme 9). Thermodynamic data for the formation of the cationic *trans*- and *cis*-$\mathbf{2}^+$ complexes in DMF at 25 °C (for the definition of K_0K_1 and K'_0K_1, see Scheme 10 and Scheme 11).

		cis-$\mathbf{1}_Z$ 4-Z (σ)[a]	K		
1		OMe (–0.268)	0.8 ± 0.1		
2		Me (–0.17)	0.9 ± 0.1		
3		H (0)	1.2 ± 0.2		
4		Cl (0.227)	1.3 ± 0.1		
5		NO_2 (0.778)	0.8 ± 0.1		
	Precursor L = PPh_3	4–Z		k_{obs} (s^{-1})	K_0K_1 (M)
6	$Pd^0(dba)L_2$	OMe		n.d.[b]	n.d.[b,c]
7	$Pd^0(dba)L_2$	Me		$6.5(\pm0.1)\times10^{-5}$	1.5×10^{-5}
8	$Pd^0(dba)L_2$	H		$1.7(\pm0.1)\times10^{-4}$	$7.9(\pm0.5)\times10^{-6}$
9	$Pd^0(dba)L_2$	Cl		$1.7(\pm0.1)\times10^{-4}$	n.d.[b]
10	$Pd^0(dba)L_2$	NO_2		$4.5(\pm0.1)\times10^{-3}$	1.0
				k_{obs} (s^{-1})	K'_0K_1 (M)
1	Pd^0L_4	OMe		$1.0(\pm0.1)\times10^{-3}$	n.d.[b]
12	Pd^0L_4	Me		$1.0(\pm0.1)\times10^{-3}$	n.d.[b]
13	Pd^0L_4	H		$2.2(\pm0.1)\times10^{-3}$	2.4×10^{-5}
14	Pd^0L_4	Cl		$3.8(\pm0.1)\times10^{-3}$	3.1×10^{-4}
15	Pd^0L_4	NO_2		n.d.[b]	n.d.[b]

[a] σ: *para* Hammett constant. [b] N.d.: not determined. [c] K_0K_4 was determined instead (see text).

(Figure S5a), the plot of $x^2(1+x)/(n-x)$ vs. $(1-x)$ was not linear as expected (vide supra for *cis*-$\mathbf{1}_H$). This suggests that the equilibrium did not involve the formation of the cationic complex *trans*-$\mathbf{2}^+$ but presumably the neutral intermediate complex (η^2-*cis*-$\mathbf{1}_{OMe}$)$Pd^0(PPh_3)_2$ (Scheme 12). We have already reported kinetic and structural evidences for the formation of such intermediate neutral complexes in acyclic allylic acetates.[13]

$$Pd^0(dba)L_2 \overset{K_0}{\rightleftharpoons} Pd^0L_2 + dba \quad L = PPh_3$$

$$cis\text{-}\mathbf{1}_{OMe} + Pd^0L_2 \overset{K_4}{\rightleftharpoons} (\eta^2\text{-}cis\text{-}\mathbf{1}_{OMe})Pd^0L_2$$

Overall equilibrium

$$cis\text{-}\mathbf{1}_{OMe} + Pd^0(dba)L_2 \overset{K_0K_4}{\rightleftharpoons} (\eta^2\text{-}cis\text{-}\mathbf{1}_{OMe})Pd^0L_2 + dba$$

Scheme 12.

Such a neutral complex might accumulate if its ionization to *trans*-$\mathbf{2}^+$ were slow. To check this hypothesis, the reaction of $Pd^0(dba)(PPh_3)_2$ with *cis*-$\mathbf{1}_{OMe}$ in DMF was monitored by conductivity measurements to detect any cationic complex.[10] A low and constant conductivity of 2.5 $\mu S \cdot cm^{-1}$ (compared to the solvent residual conductivity of 1.5 $\mu S \cdot cm^{-1}$) was observed after addition of *cis*-$\mathbf{1}_{OMe}$ (32 mM) to $Pd^0(dba)(PPh_3)_2$ (1 mM) up to 4000 s. This indicates that cationic complex *trans*-$\mathbf{2}^+$ was not generated in high concentration (vide infra for the cationic complex generated from *cis*-$\mathbf{1}_{NO2}$). Assuming that the investigated equilibrium stopped at the level of (η^2-*cis*-$\mathbf{1}_{OMe}$)$Pd^0(PPh_3)_2$ (Scheme 12), the expression of the equilibrium constant would become $K_0K_4 = x(1+x)/[(n-x)(1-x)]$. The plot of $x(1+x)/(n-x)$ vs. $(1-x)$ was indeed linear (Figure S5b) in agreement with the equation in Scheme 12. The value of $K_0K_4 = 0.025$ (DMF, 25 °C) was determined from the corresponding slope. The fact that the formation of the cationic complex *trans*-$\mathbf{2}^+$ from (η^2-*cis*-$\mathbf{1}_{OMe}$)$Pd^0(PPh_3)_2$ was extremely slow explains why the isomerization *cis*-$\mathbf{1}_{OMe}$ to *trans*-$\mathbf{1}_{OMe}$ in the presence of $Pd^0(dba)(PPh_3)_2$ was the slowest one observed (Figure 4).[14]

When considering *cis*-$\mathbf{1}_{NO2}$, which possesses a better leaving group than *cis*-$\mathbf{1}_{OMe}$ (4-NO_2–C_6H_4-CO_2^- > 4-MeO–C_6H_4-CO_2^-), the conductivity of the solution did increase over time to reach a final conductivity of 16 $\mu S \cdot cm^{-1}$ by reacting *cis*-$\mathbf{1}_{NO2}$ (32 mM) with $Pd^0(dba)(PPh_3)_2$ (1 mM) in DMF at 25 °C (Figure S6). This experiment showed that the cationic complex $\mathbf{2}^+$ was indeed formed from *cis*-$\mathbf{1}_{NO2}$, which was more reactive than *cis*-$\mathbf{1}_{OMe}$ in both the complexation and the ionization steps.

From the values of k_{obs} collected in Table 1, one observes that for a given Z, the isomerization of *cis*-$\mathbf{1}_Z$ to *trans*-$\mathbf{1}_Z$ is always faster when catalyzed by $Pd^0(PPh_3)_4$ than by $Pd^0(dba)_2 + 2PPh_3$, in chloroform. These data confirm that: i) the oxidative addition in which the cationic complexes are formed is reversible, and ii) the isomerization process depends on the structure of the Pd^0 precursor i.e., on the concentration of the active $Pd^0(PPh_3)_2$ complex. This shows that the overall isomerization proceeds through the reversible isomerization of the cationic complexes via an S_N2 mechanism induced by $Pd^0(PPh_3)_2$ (Scheme 7), as established by Bäckvall et al. in a related series of cationic complexes (CO_2Me instead of Ph substituted on the cycle).[5e]

For a given precursor, one sees that the isomerization of *cis*-$\mathbf{1}_Z$ to *trans*-$\mathbf{1}_Z$ is faster when Z is a better electron withdrawing group in the order $NO_2 > Cl > H > Me > OMe$ (compare k_{obs} in entries 6–10, entries 11–15 in Table 1). In other words, the better the leaving group 4-Z-C_6H_4-CO_2^-, the faster the isomerization is: 4-NO_2–C_6H_4-CO_2^- > 4-Cl–C_6H_4-CO_2^- > C_6H_5-CO_2^- > 4-Me–C_6H_4-CO_2^- > 4-MeO–C_6H_4-CO_2^-. This tendency is correlated with the evolution of the equilibrium constant of the formation of the cationic complex with Z (see K_0K_1 for $Pd^0(dba)(PPh_3)_2$ and K'_0K_1 for $Pd^0(PPh_3)_4$ in Table 1, determined in DMF).[14] Indeed, the better the leaving group, the higher the concentration of the cationic complex in its equilibrium with the neutral allylic benzoates, and thus the faster the isomerization of *cis*-$\mathbf{1}_Z$ to *trans*-$\mathbf{1}_Z$.

Conclusions

In chloroform, the reactions of cyclic allylic *para*-Z-substituted benzoates *cis*-$\mathbf{1}_Z$ with Pd^0 complexes generated from the precursors $Pd^0(PPh_3)_4$ or [$Pd^0(dba)_2 + 2PPh_3$] are reversible and proceed with isomerization at the allylic position to give *trans*-$\mathbf{1}_Z$. This isomerization is a consequence of the isomerization of the cationic (η^3-allyl)$Pd(PPh_3)_2^+$ complex through an S_N2 mechanism induced by the species $Pd^0(PPh_3)_2$. The rate of isomerization depends on the catalytic precursor {$Pd^0(PPh_3)_4$ > [$Pd^0(dba)_2 + 2PPh_3$]} in agreement with the S_N2 mechanism, since the concentration of $Pd^0(PPh_3)_2$ is about 10 times less in the second case than in the first, for an identical overall catalyst concentration. The *para*-substituent Z on the phenyl group of the benzoate has been modified to examine the effect of the leaving group on the rate of the isomerization process. The rate of isomerization follows the same order as the leaving group properties: 4-NO_2–C_6H_4–CO_2^- > 4-Cl–C_6H_4–CO_2^- > C_6H_5–CO_2^- > 4-Me–C_6H_4-CO_2^- > 4-MeO–C_6H_4-CO_2^-. From the determination of the equilibrium constant between the neutral *cis*-$\mathbf{1}_Z$ and the cationic complex in DMF, it also comes out that under identical experimental conditions, the higher the concentration of the cationic complex, the faster the isomerization of *cis*-$\mathbf{1}_Z$ to *trans*-$\mathbf{1}_Z$.

In a real catalytic reaction, a competition may occur at the level of the cationic (η^3-allyl)palladium complex between the re-entrance of the leaving group and the attack of the nucleophile. This would be accentuated for poor nucleophiles. This competition should be more in favor of the attack of the leaving group, viz. in favor of the isomerization, as the catalytic reaction proceeds because the concentration of the leaving group increases while that of the nucleophile decreases during the course of the catalytic reaction. Therefore, the leaving group cannot be considered as a "spectator and innocent" species because of the reversibility of the oxidative addition and its ensuing influence on the rate of the isomerization processes. The structure of the

catalytic precursor is not innocent either, since its choice determines the concentration of the key intermediate Pd^0L_2 and therefore affects the rate of the competitive isomerization. This appears to be a likely origin of the lack of stereospecificity observed in catalytic reactions. A pertinent choice of the leaving group and the catalytic precursor should therefore allow optimization of the overall competition and therefore improve the stereospecificity of the nucleophilic substitution.

Experimental Section

General: ^1H and ^{13}C NMR spectra were recorded with a Bruker AC-250 MHz spectrometer with tetramethylsilane as an internal standard. UV spectra were recorded with an mc² Safas Monaco spectrometer. Conductivity measurements were performed with a Tacussel CDM210 conductivity meter (cell constant: 1 cm^{-1}). All experiments were performed under Ar.

Chemicals: DMF was distilled from calcium hydride under vacuum and kept under argon. $CDCl_3$, dba, and PPh_3 were commercial. $Pd^0(dba)_2$,[15] *cis*-5-phenylcyclohex-2-enol,[15] and *cis*-5-phenylcyclohex-2-enyl benzoate[16] were prepared as described in the literature.

General Procedure for the Synthesis of *cis*-5-Phenylcyclohex-2-enyl 4-Z-Benzoate: *cis*-5-Phenylcyclohex-2-enol (3 mmol) was treated with a 4-Z-benzoyl chloride (1.1 equiv.) in the presence of DMAP (0.1 equiv.) and Et_3N (1.2 equiv.) in Et_2O (10 mL). The reaction mixture was stirred at room temperature overnight, diluted with 20 mL of diethyl ether, and washed successively with 1 M aqueous HCl and saturated Na_2CO_3. The organic phase was dried with $MgSO_4$ and concentrated. The crude product was purified by flash chromatography (silica, heptane/ethyl acetate: 8:2) to give the corresponding 4-substituted benzoate.

***cis*-5-Phenylcyclohex-2-enyl 4-Methoxybenzoate** was obtained in 90% yield as white crystals. m.p. 68 °C. ^1H NMR (250 MHz, $CDCl_3$): δ = 1.98 (td, J = 12, 10 Hz, 1 H), 2.15–2.55 (m, 3 H), 2.95–3.15 (m, 1 H), 3.86 (s, 3 H), 5.7–5.85 (m, 2 H), 5.95–6.05 (m, 1 H), 6.91 (d, J = 9 Hz, 2 H), 7.15–7.4 (m, 5 H), 7.99 (d, J = 9 Hz, 2 H) ppm. ^{13}C NMR (62.9 MHz, $CDCl_3$): δ = 166.2, 163.4, 145.3, 131.8, 130.5, 128.7, 127.5, 126.9, 126.6, 123.0, 113.7, 71.3, 55.6, 39.1, 35.4, 33.6 ppm. IR: $\tilde{\nu}_{CO}$ = 1705 cm^{-1}. HRMS $C_{20}H_{20}O_3$: calcd. 308.1407; found 308.1416. $C_{20}H_{20}O_3$ (308): calcd. C 77.90, H 6.54; found C 77.93, H 6.59.

***cis*-5-Phenylcyclohex-2-enyl 4-Methylbenzoate** was obtained in 92% yield as white crystals. m.p. 53 °C. ^1H NMR (250 MHz, $CDCl_3$): δ = 1.98 (td, J = 12, 10 Hz, 1 H), 2.15–2.55 (m, 3 H), 2.40 (s, 3 H), 2.95–3.15 (m, 1 H), 5.7–5.85 (m, 2 H), 5.95–6.05 (m, 1 H), 7.05–7.4 (m, 7 H), 7.93 (d, J = 8 Hz, 2 H) ppm. ^{13}C NMR (62.9 MHz, $CDCl_3$): δ = 166.5, 145.3, 143.7, 130.5, 129.8, 129.2, 128.7, 127.9, 127.4, 126.9, 126.6, 71.4, 39.1, 35.4, 33.6, 21.8 ppm. IR: $\tilde{\nu}_{CO}$ = 1708 cm^{-1}. HRMS $C_{20}H_{20}O_2$: calcd. 292.1458; found 292.1467. $C_{20}H_{20}O_2$ (292): calcd. C 82.16, H 6.89; found C 82.32, H 6.91.

***cis*-5-Phenylcyclohex-2-enyl 4-Chlorobenzoate** was obtained in 98% yield as white crystals. m.p. 74 °C. ^1H NMR (250 MHz, $CDCl_3$): δ = 1.99 (td, J = 12, 10 Hz, 1 H), 2.15–2.55 (m, 3 H), 2.95–3.15 (m, 1 H), 5.7–5.85 (m, 2 H), 5.95–6.05 (m, 1 H), 7.1–7.45 (m, 5 H), 7.40 (d, J = 8 Hz, 2 H), 7.96 (d, J = 8 Hz, 2 H) ppm. ^{13}C NMR (62.9 MHz, $CDCl_3$): δ = 165.4, 145.0, 139.3, 131.1, 130.8, 129.0, 128.7, 128.6, 126.9, 126.8, 126.5, 71.8, 38.9, 35.2, 33.4 ppm. IR: $\tilde{\nu}_{CO}$ = 1713 cm^{-1}. HRMS $C_{19}H_{17}ClO_2$: calcd. 312.0912; found 312.0895. $C_{19}H_{17}ClO_2$ (312): calcd. C 72.96, H 5.48; found C 73.32, H 5.65.

***cis*-5-Phenylcyclohex-2-enyl 4-Nitrobenzoate** was obtained in 84% yield as pale yellow crystals. m.p. 85 °C. ^1H NMR (250 MHz, $CDCl_3$): δ = 2.03 (td, J = 12 and 10 Hz, 1 H), 2.15–2.55 (m, 3 H), 2.95–3.15 (m, 1 H), 5.7–5.85 (m, 2 H), 5.95–6.05 (m, 1 H), 7.1–7.4 (m, 5 H), 8.18 (d, J = 9 Hz, 2 H), 8.28 (d, J = 9 Hz, 2 H). ^{13}C NMR (62.9 MHz, $CDCl_3$): δ = 164.4, 150.5, 144.9, 135.9, 131.3, 130.7, 128.6, 126.8, 126.6, 126.4, 123.5, 72.6, 38.8, 35.1, 33.2. IR: $\tilde{\nu}_{CO}$ = 1720 cm^{-1}. HRMS $C_{19}H_{17}NO_4$: Calcd. 323.1152; found: 323.1163. $C_{19}H_{17}NO_4$ (323): calcd. C 70.58, H 5.30; found C 70.42; H 5.35.

Typical Procedure for UV Experiments: From a stock solution of DMF (10 mL) containing $Pd^0(dba)_2$ (5.7 mg, 10 μmol) and PPh_3 (5.4 mg, 20 μmol), a 300 μL aliquot was transferred under Ar to the thermostatted UV cell (1 mm length) and a UV measurement was performed. It was followed by successive additions of known amounts of *cis*-$\mathbf{1}_Z$ (see *n* in Figure 3) from a stock solution (0.3 M in DMF). The UV measurement was performed immediately after hand-shaking the cell. From a stock solution of DMF (10 mL)containing $Pd^0(PPh_3)_4$ (11.5 mg, 10 μmol), a 300 μL aliquot was transferred under Ar to the thermostatted UV cell (1 mm length) and a UV measurement was performed. It was followed by successive additions of known amounts of *cis*-$\mathbf{1}_Z$ (see *n* in Figure 3) from a stock solution (0.3 M in DMF). The UV measurement was performed immediately after hand-shaking the cell.

Typical Procedure for Conductivity Measurements: To a thermostatted cell connected to a Schlenk line and containing a solution of $Pd^0(dba)_2$ (5.7 mg, 10 μmol) and PPh_3 (5.3 mg, 20 μmol) in DMF (10 mL) was added *cis*-$\mathbf{1}_{OMe}$ (98.4 mg, 320 μmol). The conductivity was recorded over time using a computerized home-made program. In another experiment, *cis*-$\mathbf{1}_{NO2}$ (103.4 mg, 320 μmol) was added to the solution of the Pd^0 complex, and the measurement was repeated.

Typical Procedure for the Kinetics of Isomerization of *cis*-$\mathbf{1}_Z$ to *trans*-$\mathbf{1}_Z$, as Followed by ^1H NMR Experiments: In an NMR tube containing $Pd^0(dba)_2$ (5.7 mg, 10 μmol), PPh_3 (5.3 mg, 20 μmol), *cis*-$\mathbf{1}_H$ 5.6 mg (20 μmol) was added, followed by of $CDCl_3$ (0.5 mL). ^1H NMR was performed vs. time up to equilibrium. To an NMR tube containing $Pd^0(PPh_3)_4$ (11.5 mg, 10 μmol) was added *cis*-$\mathbf{1}_{Cl}$ (6.3 mg, 20 μmol) followed by $CDCl_3$ (0.5 mL). ^1H NMR was performed vs. time up to equilibrium.

Supporting Information: Graphs for the determination of equilibrium and rate constants.

Acknowledgments

This work has been supported in part by the Centre National de la Recherche Scientifique (UMR CNRS-ENS-UPMC 8640) and the Ministère de la Recherche (Ecole Normale Supérieure). We thank Johnson Matthey for a generous loan of sodium tetrachloropalladate.

[1] a) S. A. Godleski, in: *Comprehensive Organic Synthesis, vol. 4* (Eds: B. M. Trost, I. Pflemming, M. F Semmelhack) Pergamon, Oxford, **1991**; b) C. G. Frost, J. Howard, J. M. J. Williams, *Tetrahedron: Asymmetry* **1992**, *3*, 1089; c) J. Tsuji, *Palladium Reagents and catalysts*, John Wiley & Sons, Chichester, **1996**, p. 290; d) B. M. Trost, D. L. Van Kanken, *Chem. Rev.* **1996**, *96*, 395; e) G. Consiglio, R. Waymouth, *Chem. Rev.* **1989**, *89*, 257; f) T. Hayashi, *Pure Appl. Chem.* **1988**, *60*, 7; g) M.

Sawamura, Y. Ito, *Chem. Rev.* **1992**, *92*, 857; h) A. Pfaltz, *Acc. Chem. Res.***1993**, *26*, 339; i) P. S. Pregosin, R. Salzman, *Coord. Chem. Rev.* **1996**, *155*, 36; j) G. Helmchen, A. Pfaltz, *Acc. Chem. Res.* **2000**, *33*, 336.

[2] a) J.-E. Bäckvall, R. E. Nordberg, *J. Am. Chem. Soc.* **1981**, *103*, 4959; b) B. Åkermark, A. Jutand, *J. Organomet. Chem.* **1981**, *217*, C41; c) J.-E. Bäckvall, R. E. Nordberg, K. Zetterberg, B. Åkermark, *Organometallics* **1983**, *2*, 1625.

[3] J. C. Fiaud, J. Y. Legros, *J. Org. Chem.* **1987**, *52*, 1907.

[4] a) B. M. Trost, T. R. Verhoeven, J. F. Fortunak, S. M. McElvain, *Tetrahedron Lett.* **1979**, 2301; b) B. M. Trost, T. R. Verhoeven, *J. Am. Chem. Soc.* **1980**, *102*, 4730.

[5] For postulated and established S_N2 mechanism, see: a) T. Takahashi, Y. Jinbo, K. Kitamura, J. Tsuji, *Tetrahedron Lett.* **1984**, *25*, 5921; b) P. B. Mackenzie, J. Whelan, B. Bosnich, *J. Am. Chem. Soc.* **1985**, *107*, 2046; c) H. Kurosawa, S. Ogoshi, N. Chatani, Y. Kawasaki, S. Murai, I. Ikeda, *Chem. Lett.* **1990**, 1745; d) J.-E. Bäckvall, K. L. Granberg, A. Heumann, *Isr. J. Chem.* **1991**, *31*, 17; e) K. L. Granberg, J.-E. Bäckvall, *J. Am. Chem. Soc.* **1992**, *114*, 6858; f) C. Amatore, S. Gamez, A. Jutand, G. Meyer, M. Moreno-Mañas, L. Morral, R. Pleixats, *Chem. Eur. J.* **2000**, *6*, 3372.

[6] a) J. C. Fiaud, J. Y. Legros, *J. Org. Chem.* **1990**, *55*, 4840; b) K. Hiroi, J. Abe, *Tetrahedron Lett.* **1990**, *31*, 3623; c) K. Hiroi, M. Haraguchi, Y. Masuda, J. Abe, *Chem. Lett.* **1992**, 2409; d) J. Y. Legros, J. C. Fiaud, *Tetrahedron* **1994**, *50*, 465.

[7] a) C. Amatore, A. Jutand, F. Khalil, M. A. M′Barki, L. Mottier, *Organometallics* **1993**, *12*, 3168; b) C. Amatore, A. Jutand, *Coord. Chem. Rev.* **1998**, *178–180*, 511; c) The formation of the complex $Pd(dba)(PPh_3)_2$ is quantitative in the reaction of $Pd(dba)_2$ with 2 equiv. of PPh_3.[7a,7b]

[8] a) The straight line does not go through zero due to an *S*-shaped curve at short time (see Figure 1, b); b) The value of K_0 was determined in DMF at 25 °C by performing UV spectroscopy on the complex $Pd^0(dba)(PPh_3)_2$ generated from $Pd^0(dba)_2$ and 2 equiv. PPh_3 in DMF. The absorbance D of $Pd^0(dba)(PPh_3)_2$ at λ = 400 nm was measured for different concentrations C_0 of $Pd^0(dba)_2$ in the range 2×10^{-5}–10^{-3} M. The value of $D = \varepsilon l C_0 - \varepsilon l K_0$ was plotted vs. C_0. $K_0 = 1.5\times10^{-5}$ M could be determined from the ratio of slope and intercept of the resulting straight line. The value of the concentration of Pd^0L_2 (L = PPh_3) in the equilibrium in Scheme 5 could be estimated from the value of K_0, considering the overall Pd^0 concentration (C_0 = 20 mM) used in the NMR study. Thus $[Pd^0L_2]_{equil5} = 1.5\times10^{-5}$ M (DMF, 25 °C, Scheme 5); c) The values of k_+ and k_- could be estimated using the concentration of $[Pd^0L_2]_{equil5}$ determined in DMF at 25 °C, although the solvent is slightly different ($CDCl_3$ instead of DMF), by using the value of $k_+ + k_- = k_{obs}/[Pd^0L_2]_{equil5}$ associated to $K = k_+/k_-$ = 1.17 (determined in $CDCl_3$ at 25 °C, vide supra). One estimated: k_+ = 5.4 $M^{-1}s^{-1}$ and k_- = 4.6 $M^{-1}s^{-1}$ (25 °C); d) For Z = Me, $k_+ = 2.1\pm0.1$ $M^{-1}s^{-1}$ and $k_- = 2.3\pm0.1$ $M^{-1}s^{-1}$. For Z = Cl, $k_+ = 6.3\pm0.1$ $M^{-1}s^{-1}$ and $k_- = 4.9\pm0.1$ $M^{-1}s^{-1}$. For Z = NO_2, $k_+ = 133\pm1$ $M^{-1}s^{-1}$ and $k_- = 166\pm1$ $M^{-1}s^{-1}$.

[9] C. Amatore, A. Jutand, G. Meyer, *Inorg. Chim. Acta* **1998**, *273*, 76.

[10] For the use of conductivity measurements for the determination of mechanisms, see: A. Jutand, *Eur. J. Inorg. Chem.* **2003**, 2017.

[11] C. Amatore, A. Jutand, G. Meyer, L. Mottier, *Chem. Eur. J.* **1999**, *5*, 466.

[12] For the effect of leaving group on the equilibrium constant, see also: N. Agenet, C. Amatore, S. Gamez, H. Gérardin, A. Jutand, G. Meyer, C. Orthwein, *ARKIVOC*, **2002**, 92. http://www.arkat-usa.org.

[13] a) C. Amatore, S. Gamez, A. Jutand, *Chem. Eur. J.* **2001**, *7*, 1273; b) C. Amatore, A. A. Bahsoun, A. Jutand, L. Mensah, G. Meyer, L. Ricard, *Organometallics* **2005**, *24*, 1569.

[14] DMF was used as solvent instead of $CHCl_3$ because it allows the observation of cationic complexes $\mathbf{2}^+$ by conductivity measurements (see Figure S6), whereas ions pairs are produced in $CHCl_3$.

[15] Y. Takahashi, Ts. Ito, Y. Ishii, *J. Chem. Soc., Chem. Commun.* **1970**, 1065.

[16] a) F. Gauchet, M. Julia, H. Mestdagh, C. Rolando, *Bull. Soc. Chim. Fr.* **1987**, 1036; b) E. Dunkelblum, R. Levene, J. Klein, *Tetrahedron* **1972**, *28*, 1009.

Received: September 19, 2005
Published Online: December 13, 2005

